

XI. TRANSISTOR AND DIODE STUDIES*

Prof. H. J. Zimmermann
Prof. R. B. Adler
Prof. S. J. Mason

Dr. W. D. Jackson
C. R. Hurtig

A. Lipsky
R. B. Martindale
R. E. Nelson

A. DIELECTRIC MODULATORS

1. Introduction

The study of balanced modulators (for dc-to-ac conversion) that employ voltage-sensitive capacitances continues. The transition capacitance of semiconductor junction diodes is voltage-sensitive and follows a law given by

$$C = C_0(v + \phi_0)^{-1/n}$$

where ϕ_0 is the contact potential, v is the instantaneous voltage across the diode, and n is a number between 2 and 3, depending on the diode construction. Silicon diodes were chosen in preference to germanium because the shunt conductance of a silicon diode at zero or reverse bias is considerably smaller than that of germanium. The capacitance of a silicon diode is only slightly dependent on temperature. A typical temperature coefficient is approximately 650 ppm/°C (see Quarterly Progress Report, April 15, 1957, p. 121). One advantage of a modulator with variable reactive elements (1) is the possibility of obtaining power gain. This factor may be important from the standpoint of noise.

Two different variable-capacitance modulators were built – one employing tuned circuits and one employing an RC bridge.

2. Tuned Modulator

The circuit diagram of the tuned modulator (2) is shown in Fig. XI-1. The circuit is driven by a balanced transformer T_1 and employs two series-tuned circuits. The currents flowing in the tuned circuits with no modulating voltage are made equal in amplitude and 180° out of phase. The two currents are added in the output transformer T_2 , which matches the modulator-output impedance to the input impedance of the amplifier. The diodes are polarized so that the capacitances of the diodes vary in opposite directions in the presence of modulating voltage. The vector diagram illustrating the operation of the modulator is shown in Fig. XI-2. The currents i_1 and i_2 are shown in the vector diagram as a function of the capacitance of the diodes. The

*This research was supported in part by Purchase Order DDL-B187 with Lincoln Laboratory, which is supported by the Department of the Army, the Department of the Navy, and the Department of the Air Force under Contract AF19(122)-458 with M. I. T.

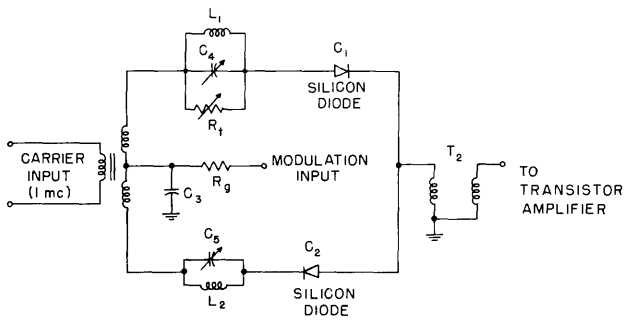


Fig. XI-1. Circuit diagram of tuned modulator.

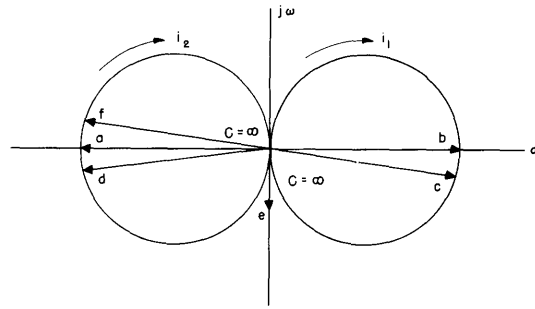


Fig. XI-2. Vector diagram of currents in the tuned circuits of the tuned modulator.

arrows denote increasing capacitance. If the tuned circuits are identical, then points on the two loci are symmetrical with respect to the origin. The normal operating point is given by the resonance condition. For carrier voltages across the diode of less than 50 mv rms, the capacitance variation with modulating voltage may be approximated as a simple linear function. With no modulation signal, the output current is the sum of vectors a and b, which is adjusted to a zero balance. When a positive modulating signal is applied, the capacitance of C_1 increases and the capacitance of C_2 decreases. The output current is the sum of vectors c and d; it is shown as vector e, which is 90° out of phase with the applied carrier signals.

With this arrangement, modulators with power gains (ratio of sideband output power to modulating signal power at the input terminals) as high as 20 db have been built. Since the components in the bridge are not identical, thermal variations impose a limit on the balance of the circuit. The amount of unbalance of the circuit is determined by the differential change in the resonant frequency and Q of the two tuned circuits. These differential factors are a function of the differences in the temperature coefficients of the components that comprise the tuned circuit. With only a reasonable choice of components, a minimum detectable signal power of the order of 10^{-16} watt and an input impedance to the modulating signal of 100 megohms can be achieved for short periods in a laboratory environment. This is equivalent to a minimum detectable current of 10^{-12} amp and 100×10^{-6} volt. To achieve a minimum detectable current of this order of magnitude over a temperature range of 10°C , components with temperature coefficients differing by less than 15 ppm/ $^\circ\text{C}$ must be chosen.

3. RC Bridge Modulator

The circuit diagram of an RC bridge modulator is shown in Fig. XI-3. This circuit was designed to minimize the effects of temperature variation. There are, essentially, only four components whose temperature coefficients must be matched – two diodes and

(XI. TRANSISTOR AND DIODE STUDIES)

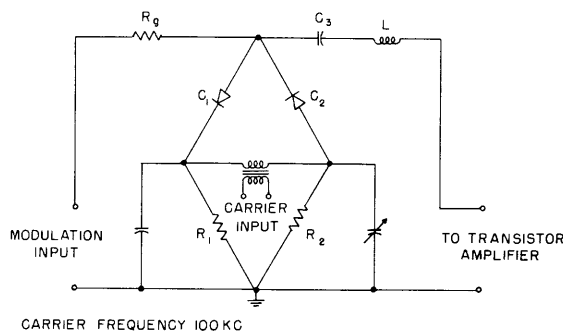


Fig. XI-3. Circuit diagram of RC bridge modulator.

two resistors. Furthermore, the temperature coefficients of the ratio of capacitors and the ratio of resistors should be equal. The simplest means of achieving this equality is to make the temperature coefficients of the resistors equal and the temperature coefficients of the capacitors equal. Precision wirewound resistors with a temperature coefficient of 25 ppm/°C are employed. In the initial design diodes were chosen for approximately equal capacitance and not for temperature coefficient. The temperature coefficient of the diode capacitance is approximately 650 ppm/°C with a variation of ± 60 ppm/°C.

Operation of the bridge is based on a change in the average value of the capacitance as a function of the modulation signal. If the carrier signal is small, so that the capacitance of the diode is a linear function of voltage, the power gain of the bridge with a conjugate match at the output is given by

$$\text{Power gain} \approx \frac{e_c^2}{16\phi^2} \frac{R_L R_g}{(R_L + R_p)^2}$$

where e_c is the rms value of the carrier voltage, ϕ is the contact potential, R_L is the load resistance, R_g is the real part of the generator resistance at the modulation frequency, and R_p is the parallel combination of the bridge resistors R_1 and R_2 . Thus, with a conjugate match the gain is independent of the value of the diode capacitance and operating frequency. For a generator resistance of 100 megohms and the values shown in Fig. XI-3, the carrier voltage must be approximately 50 mv rms to achieve a power gain of 10. This carrier level is so large that the approximations that were made are questionable. To achieve higher gains with lower carrier levels, the bridge resistors and load impedance should be greatly reduced.

Over a laboratory temperature range of a few degrees centigrade, we have been able to maintain a balance that is less than an equivalent input voltage of $\pm 40 \times 10^{-6}$ volt

(XI. TRANSISTOR AND DIODE STUDIES)

with a 100-megohm input impedance. The balance is below the thermal noise and shot noise of the system. Thermal noise for this system, which has a 1000-cps bandwidth, is approximately 10^{-17} watt.

This balance has been maintained over the laboratory temperature range for generator resistances of 100,000 ohms to 10 megohms. The noise figure of the converter and amplifier was not accurately measured. Both i-f noise and converter noise contribute to the noise at the output. We have not yet determined whether modulatory noise of the capacitors exists.

A more careful design will be made in order to achieve the best compromise between noise figure (random) and bridge unbalance caused by thermal variations. It should be noted that the input resistance of the bridge at the modulation input is determined by the resistance of silicon diodes at, or close to, zero bias. This resistance is an exponential function of temperature. If temperature control is necessary in some applications, there is considerable advantage in using a cooling system rather than an oven. Another factor to be considered is the use of reverse bias on the diodes. With reverse bias, higher input impedance levels might be obtained and the carrier signals can be increased. Both of these factors would yield a higher power gain. The disadvantage of employing reverse bias is the requirement that the differential change in bias on the diodes be small compared with the equivalent drift signals or noise signals.

C. R. Hurtig

References

1. J. M. Manley and H. E. Rowe, Some general properties of nonlinear elements, Proc. IRE 44, 904-913 (1956).
2. A. H. Lipsky, A d-c to a-c converter using the capacity of a reversed biased p-n junction, S. M. Thesis, Department of Electrical Engineering, M.I.T., May 1957.

B. CRYSTAL ADMITTANCE MEASUREMENTS

A method for determining the spreading resistance of point-contact crystal rectifiers was outlined in the Quarterly Progress Report of April 15, 1957, page 124. The method requires that the curve of incremental resistance against bias coincide with the corresponding curve for an ideal barrier in the region of zero bias. This condition has not been found to exist in 1N21, 1N23B, and 1N25 silicon crystal rectifiers. The incremental-resistance curve for the 1N25 crystal rectifier shown in Fig. XI-4 was obtained by bridge measurement at 1 kc.

The failure of these curves to exhibit properties expected of PN junction diodes and known to obtain in some point-contact diodes (e. g. , "bonded" diodes) makes the assumption that the barrier in silicon microwave crystals can be described in terms

(XI. TRANSISTOR AND DIODE STUDIES)

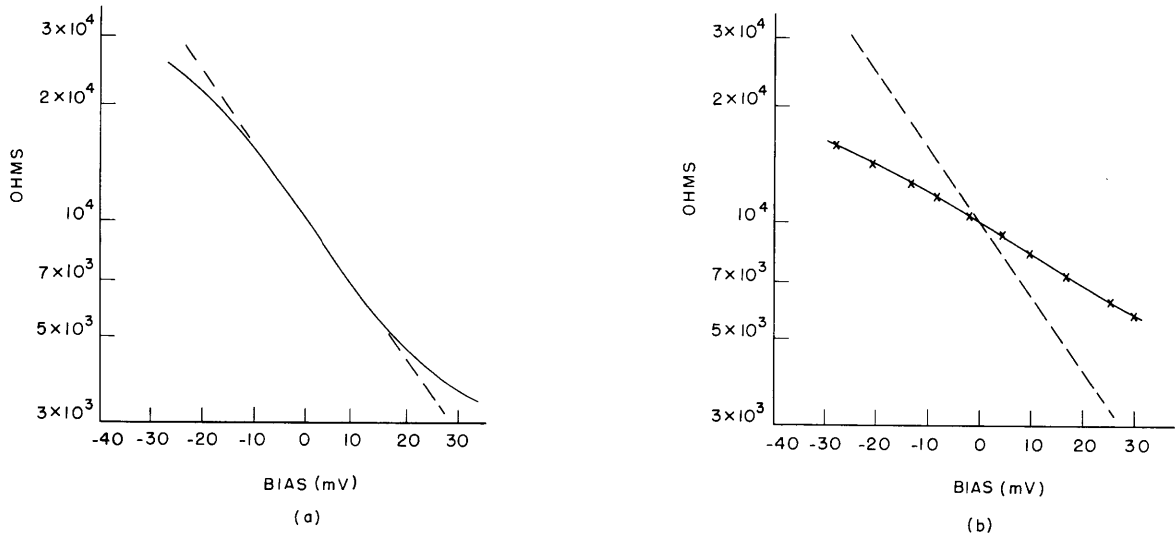


Fig. XI-4. Incremental resistance as a function of bias (ideal PN junction relation is shown by dashed line): (a) typical bonded diode; (b) type 1N25 crystal rectifier.

of PN-junction theory questionable. On the basis of this assumption, the spreading resistance would be nonlinear with bias from conductivity modulation, and frequency-dependent because of diffusion effects in the barrier action. However, if diffusion were, at most, a secondary effect, the spreading resistance would be constant and independent of frequency over the range that is of interest (up to 10 kmc) which lies below the range in which dielectric relaxation effects may become important.

Figure XI-5a shows the small-signal, lumped-parameter, equivalent-circuit model used for these investigations, and Fig. XI-5b gives a series representation of the experimental data after subtraction of the external capacitance and whisker inductance. With reverse bias that is more negative than approximately 0.25 volt, it seems reasonable to expect that a high-frequency range can be found in which $R_b \gg 1/\omega C_b$, and consequently $R_e \approx R_s$; $X_e \approx 1/\omega C_b$. From this point of view, the available data have been used to make an estimate of the spreading resistance for each of the crystal rectifiers mentioned above. With this value of R_s , and with the assumption of negligible diffusion effect at the barrier, the variation of the small-signal barrier resistance and capacitance over the bias range 0.3 to -0.5 volt at frequencies of 1 kc and 10, 300, 1000, and 3000 mc has been computed; the results for the 1N25 crystal rectifier are shown in Figs. XI-6 and 7. The form of the curves for the other two rectifiers is similar.

The curves agree well with the requirements of the known microwave mixing performance of unformed silicon crystal rectifiers. The R_b behavior in the direction of

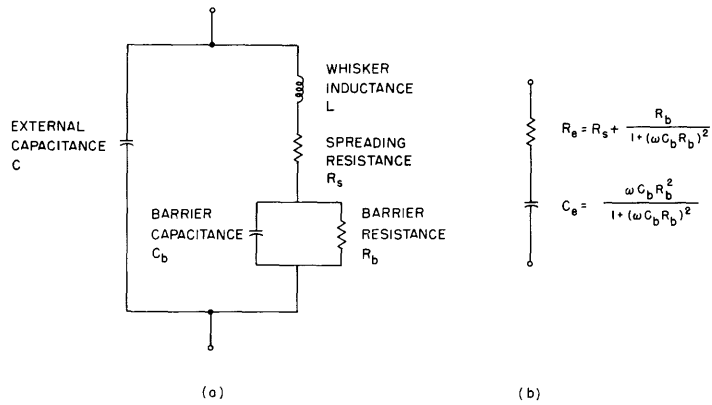


Fig. XI-5. Small-signal equivalent circuit models: (a) complete model; (b) series representation of R_s , R_b , and C_b .

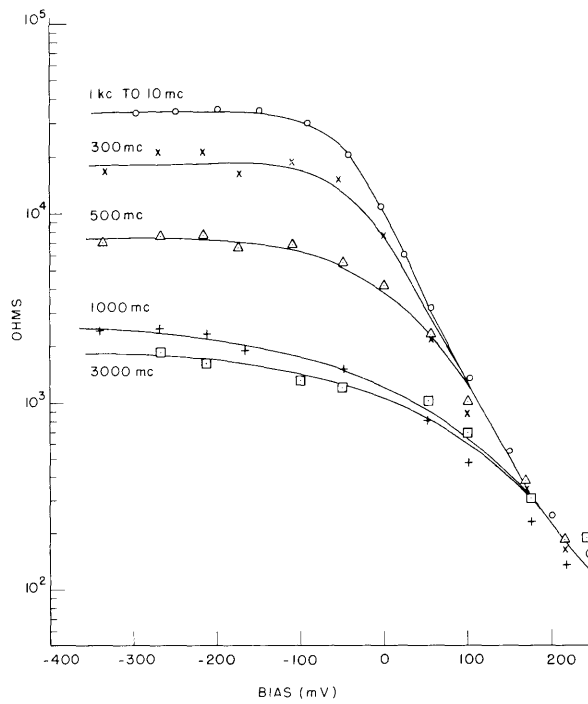


Fig. XI-6. Small-signal barrier resistance as a function of bias for type 1N25 crystal rectifiers.

(XI. TRANSISTOR AND DIODE STUDIES)

forward bias is independent of frequency to the limit of recommended operating frequency f_m , while the reduction of R_b with increasing frequency in reverse bias may be caused by frequency-dependent surface effects. The barrier capacitance C_s is

Table XI-1. Evaluation of the $2\pi f_m C_b R_s$ product for several crystal rectifiers.

Type	R_s (ohms)	C_b (zero bias) ($\mu\mu\text{f}$)	f_m (kmc)	$2\pi f_m C_b R_s$
1N21	8	0.42	3	0.063
1N23B	6	0.19	10	0.071
1N25	3.3	2.55	1	0.054

independent of frequency and its relation to the bias voltage V is of the form $C_b = A/(V_o - V)^{1/2}$ for both forward and reverse bias, where A and V_o are constants. The criterion that $2\pi f_m R_s C_b \gg 1$ for good mixing performance has long been established, and Table XI-1 shows it to be confirmed by the computed results. In the light of this experimental evidence it seems reasonable to conclude that the point-contact silicon crystals for microwave mixing developed by empirical design during the past fifteen years are "one-carrier" or "drift" devices, although further work is evidently required to establish these points. They are to be contrasted with the PN

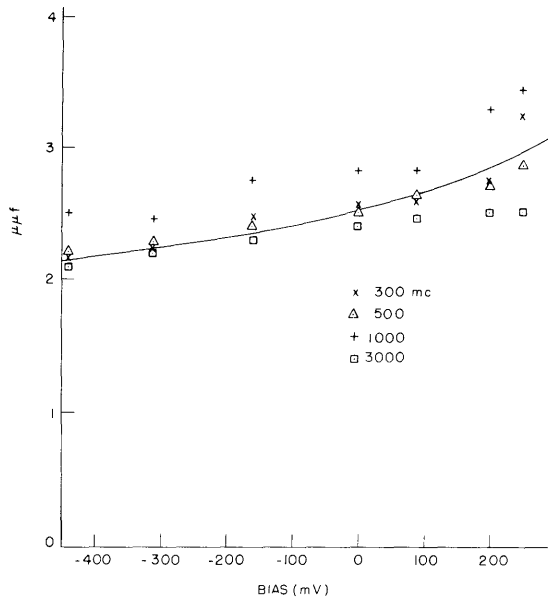


Fig. XI-7. Small-signal barrier capacitance as a function of bias for type 1N25 crystal rectifier.

(XI. TRANSISTOR AND DIODE STUDIES)

junction or "transistor-like" point-contact diodes in which diffusion plays a dominant role that are available for much lower-frequency applications than we have considered. It is known that the silicon base of microwave crystals should be heavily doped and its surface carefully treated for good mixing performance, and these conditions, which are necessary for the one-carrier case, give additional evidence to support the proposed model.

Experimental investigation is being continued with small-signal admittance measurements on a type 1N263 germanium microwave crystal to determine if this also is a one-carrier device. Measurements on point-contact diodes with static characteristics that closely approximate those predicted for an abrupt hemispherical PN junction are also contemplated.

W. D. Jackson, R. B. Martindale